

# A virtual network for estimating daily new snow water equivalent and snow depth in the Swiss Alps

Luca EGLI,<sup>1</sup> Tobias JONAS,<sup>1</sup> Jean-Marie BETTEMS<sup>2</sup>

<sup>1</sup> WSL Institute for Snow and Avalanche Research SLF, Flüelastrasse 11, CH-7260 Davos Dorf, Switzerland  
E-mail: [egli@slf.ch](mailto:egli@slf.ch)

<sup>2</sup> Federal Office of Meteorology and Climatology MeteoSwiss, CH-8044 Zürich, Switzerland

**ABSTRACT.** Daily new snow water equivalent (HNW) and snow depth (HS) are of significant practical importance in cryospheric sciences such as snow hydrology and avalanche formation. In this study we present a virtual network (VN) for estimating HNW and HS on a regular mesh over Switzerland with a grid size of 7 km. The method is based on the HNW output data of the numerical weather prediction model COSMO-7, driving an external accumulation/melting routine. The verification of the VN shows that, on average, HNW can be estimated with a mean systematic bias close to 0 and an averaged absolute accuracy of 4.01 mm. The results are equivalent to the performance observed when comparing different automatic HNW point estimations with manual reference measurements. However, at the local scale, HS derived by the VN may significantly deviate from corresponding point measurements. We argue that the VN presented here may introduce promising cost-effective options as input for spatially distributed snow hydrological and avalanche risk management applications in the Swiss Alps.

## 1. INTRODUCTION

In cryospheric sciences such as snow hydrology, avalanche formation/dynamics and snow climatology, daily new snow water equivalent (HNW, mm) and snow depth (HS, m) are important measurement categories. Together with wind speed, HNW is of significant practical importance for avalanche hazard estimation (McClung and Schaerer, 1993; Egli, 2008) and represents a key input parameter for spatially distributed snow models (e.g. Lehning and others, 2006; Liston and Elder, 2006). The monitoring and modelling of water resources, represented by HS (respectively, snow water equivalent (SWE)), is the basic aim of snow hydrology (e.g. Grayson and Blöschl, 2001; Anderton and others, 2002). In particular, estimates of the spatial and temporal distribution of HS (or SWE) are essential (Luce and others, 1998; Skaugen, 2007) for water resources management (e.g. Schaeffli and others, 2007) and flood prevention.

During the last decades, various expensive networks of manual and automatic point HS (and occasionally HNW) measurements have been set up in the Swiss Alps. Automatic methods have the advantage of providing data at high temporal resolution in terrain that is difficult to access. Durand and others (1993) presented a first analysis method for relevant meteorological parameters for snow models, while Egli and others (2009) investigated different methods to reveal a general feasibility benchmark in automatic estimation of HNW.

In this study, we present a virtual network (VN) to estimate HNW and HS on a regular grid (grid size 7 km) covering the entire Swiss Alps. The method is based on the HNW output data of the numerical weather prediction model (COSMO-7), developed by the Consortium for Small-Scale Modelling currently composed of the national weather services of Germany, Switzerland, Italy, Greece, Poland and Romania. The raw snow precipitation output of COSMO-7 drives a simple external accumulation/melting routine that allows HNW and HS to be computed for each gridcell. This routine does not account for individual physical processes (e.g.

settling of snow cover and fresh snow). Instead, it evaluates bulk accumulation and melting rates based on COSMO-7 HNW data calibrated using observed HS data from existing snow-monitoring networks.

We believe that the VN presented here may introduce promising cost-effective options as input for spatially distributed snow hydrological models and avalanche risk management applications. If a numerical weather model and HS point measurement stations are available, a VN can be developed for other mountainous regions that are not as densely instrumented as the Swiss Alps.

## 2. DATA

### 2.1. COSMO-7 model output data

A numerical weather prediction system is operated by MeteoSwiss ([www.meteoswiss.ch](http://www.meteoswiss.ch)) for a wide range of applications. This system is based on the COSMO-7 model ([www.cosmo-model.org](http://www.cosmo-model.org)), which is a primitive equation model with non-hydrostatic, fully compressible dynamics. The prognostic variables include precipitation (separated into snow and rain) and many other meteorological parameters. COSMO-7 is used in two modes: (1) a free forecast mode, where the temporal evolution of the atmosphere is computed without any constraints other than the lateral boundary conditions from the driving model (European Centre for Medium-range Weather Forecasts, [www.ecmwf.int/research](http://www.ecmwf.int/research)), and (2) an assimilation mode to produce the best gridded representation of the atmosphere by blending available current observations with the model dynamic (the so-called data assimilation process). Note that no observed precipitation is assimilated in COSMO-7. The data assimilation process is not a simple interpolation of available observations, but instead produces a consistent state of the full atmosphere.

In this study we have chosen to use data from the assimilation mode of COSMO-7 between September 2005 and February 2008. For each day, snow precipitation (i.e.

**Table 1.** Table of nomenclature

Abbreviation	Description
HNW	Daily new snow water equivalent
HS	Snow depth
HNW <sub>MEAS</sub>	Observed daily new snow water equivalent
VN.RAW	Uncorrected COSMO-7 output
VN.CORR	Corrected COSMO-7 (virtual network)
$\delta$ HNW	Systematic bias
$\sigma(\delta$ HNW)	Absolute accuracy
$R^2_{\log}$	Coefficient of correlation
POD	Probability of detection
FAR	False alarm rate

solid precipitation only) cumulated from 0000 UTC to 2400 UTC for the automatic reference stations (and from 0800 UTC to 0800 UTC on the following day for the manual reference stations) has been extracted from COSMO-7 and used to derive  $HNW_{VN,RAW}$  at the surface. Introduced abbreviations are summarized in Table 1.

## 2.2. Point measurements

For this study, 141 stations spread over the entire range of the Swiss Alps (Fig. 1) were available to provide daily measurements of HS during the period September 2005 to February 2008. The sites have been carefully selected in flat open terrain, with as little wind influence as possible, to ensure regional representativeness of the HS/HNW estimation (Egli, 2008). In order to derive HNW from HS measurements, we used a simple parameterization proposed by Egli and others (2009):

$$HNW_{MEAS}(\delta HS_{24h})(\text{mm}) = \begin{cases} 1 + 1.09 \delta HS_{MEAS,24h}(\text{cm}) & \text{for } \delta HS_{MEAS,24h} > 0 \\ 0 & \text{for } \delta HS_{MEAS,24h} \leq 0, \end{cases} \quad (1)$$

where  $\delta HS_{MEAS,24h}$  denotes the 24 hour difference between an HS reading (measured here in centimetres) and the respective observations from the previous day. Possible limitations of using Equation (1) are discussed in section 4.1. Note that for automatic measurements from the network of the Intercantonal Measurement and Information System (IMIS; see Rhyner and others, 2002), HS estimations were provided at 0000 h while manual HS readings (for observations, see Marty, 2008) were provided at around 0800 h. The values of HS were later checked for plausibility, and single missing/faulty values were corrected manually by interpolation. Finally, HNW was only calculated for the period 1 November–30 April for each season (analogous to Egli and others, 2009), while HS is considered during the entire seasons of 2005–08 if  $HS > 0$ .

## 3. METHODOLOGY

### 3.1. Virtual network (VN)

#### HNW estimated by VN

The cumulated snow precipitation output of COSMO-7 ( $HNW_{VN,RAW}$ ) constituted the basis of the VN. Thirty-five snow stations (of 141) were set aside for adjusting  $HNW_{VN,RAW}$  to measured HS ( $HNW_{MEAS}$ ). These stations are referred to as reference stations (Fig. 1, crosses), while the remaining 106 stations are referred to as control stations. All

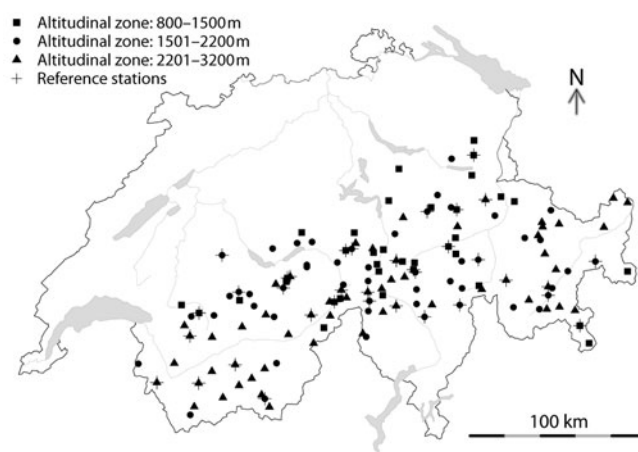


**Fig. 1.** Measurement stations: 141 point measurements of snow depths in the Alpine region over Switzerland. The stations are located at altitudes 800–3130 m a.s.l., where the three different elevation zones are indicated with squares, points and triangles. Reference stations are marked with a cross.

stations were separated into three different elevation bands (800–1500 m, 1501–2200 m and 2201–3200 m; see legend of Fig. 1).

Reference stations were selected to cover all regions and elevation bands approximately evenly, in the horizontal as well as in the vertical space. COSMO-7 mesh points were assigned to corresponding snow stations by searching the gridpoint with centre nearest to the station. The horizontal station coordinates deviated about  $\pm 2.7$  km on average (maximum  $7 \text{ km} \times \sqrt{2}/2 = 4.9 \text{ km}$ ) from the centre of  $HNW_{VN,RAW}$ , while the vertical difference between stations and respective  $HNW_{VN,RAW}$  gridcells deviated by about  $\pm 250$  m (Schaub, 2007). The VN therefore covers an area of approximately  $7 \text{ km} \times 7 \text{ km}$  on the surface (horizontal). In comparison with the point measurement stations, a vertical distension of about 500 m is provided.

The correction routine for  $HNW_{VN,RAW}$  first identified possible outliers of  $HNW_{VN,RAW}$  if  $HNW_{VN,RAW}$  exceeded the maximum of  $HNW_{MEAS}^r$  at the reference stations (index  $r$ ). Outliers were replaced by the maximum of  $HNW_{MEAS}^r$  for each elevation band. Secondly, a correction matrix  $\text{CorrMat}^r$  was calculated from the difference between  $HNW_{MEAS}$  and  $HNW_{VN,RAW}$  for each reference station and for each elevation band:

$$\text{CorrMat}^r = HNW_{MEAS}^r - HNW_{VN,RAW}^r. \quad (2)$$

For all remaining locations (index  $c$ ) of the respective elevation band, the values of the correction matrix were then interpolated by an inverse distance interpolation:

$$\text{CorrMat}^c = \frac{\sum_{i=1}^N w_i \times \text{CorrMat}^r_i}{\sum_{i=1}^N w_i}, \quad (3)$$

where

$$w_i = \frac{1}{d(|r_i - c|)} \quad (4)$$

is the inverse distance weighting function.  $d$  represents the Euclidean metric distance operator and  $N$  is the total number of reference locations ( $N = 35$  here). The corrected COSMO-7 HNW estimation for the control stations ( $HNW_{VN,CORR}^c$ ) was then defined by:

$$HNW_{VN,CORR}^c = \text{CorrMat}^c + HNW_{VN,RAW}^c, \quad (5)$$

**Table 2.** Contingency table for the validation of the HNW estimations of the virtual network. The point measurements at the control sites  $HNW_{MEAS}$  are observed and the estimations of the virtual network  $HNW_{VN}$  are forecast

HNW <sub>VN</sub> (forecast)	HNW <sub>MEAS</sub> (observed)	
	NO	YES
NO	<i>a</i>	<i>b</i>
YES	<i>c</i>	<i>d</i>

where negative values of  $HNW_{VN.CORR}^c$  were set to zero.

*HS estimation by the VN*

HS is basically calculated from the summation of HNW during the accumulation period, while a simple melting procedure is used to calculate HS during the ablation period. To calculate a temporary term  $TEMP.HS_{VN}^{cr}(t)$  for the COSMO-7 gridpoints, the values of  $HNW_{VN.CORR}^{cr}$  were added iteratively day by day:

$$TEMP.HS_{VN}^{cr}(t) = HNW_{VN.CORR}^{cr}(t) + HS_{VN}^{cr}(t - 1). \quad (6)$$

Note that instead of a simple cumulation of  $HNW_{VN.CORR}^{cr}(t)$  for each day, this iterative procedure also allows HS to be determined for snowfall events during the melting period. However, at this point  $TEMP.HS_{VN}^{cr}(t)$  does not indicate a real snow depth measure. In order to convert  $TEMP.HS_{VN}^{cr}(t)$  to corresponding HS data, we employed data from the reference stations to calibrate  $TEMP.HS_{VN}^{cr}(t)$  using a simple linear parameterization:

$$HS_{VN}^r(t) = TEMP.HS_{MEAS}^r(t) \times slope + intercept. \quad (7)$$

Again, such a parameterization was obtained for each elevation band separately. The resulting parameters of Equation (7) (slope and intercept) were subsequently used to convert  $TEMP.HS$  to HS at the control stations:

$$HS_{VN}^c(t) = TEMP.HS_{VN}^c(t) \times slope + intercept. \quad (8)$$

The above procedure was applied for all days (considered here as the period of accumulation) except during ablation, which is defined as all days if  $mean(HS_{MEAS}^r(t)) - mean(HS_{MEAS}^r(t - 4)) < 0$  and  $mean(HS_{MEAS}^r(t)) < 0.75 \times max(mean(HS_{MEAS}^r(t)))$ . Note that this criterion does not take into account any information about the physical processes of melting (e.g. liquid water content). It approximately defines the point where the mean snow depth at the reference stations for each elevation band decreases due to melting conditions (Egli and Jonas, 2009). In case of melting conditions, we calculated a melting matrix from  $HS_{MEAS}^r(t) - HS_{MEAS}^r(t - 1)$  for every elevation band at the reference stations:

$$MeltMat^r(t) = HS_{MEAS}^r(t) - HS_{MEAS}^r(t - 1). \quad (9)$$

We calculated melt rates for all remaining locations using the inverse distance weighting method, in the same way as for Equations (3) and (4):

$$MeltMat^c(t) = \frac{\sum_{i=1}^N w_i \times MeltMat^r_i(t)}{\sum_{i=1}^N w_i}, \quad (10)$$

where

$$w_i = \frac{1}{d(|r_i - c|)}. \quad (11)$$

Finally, HS (for melting conditions) was derived for the control stations as

$$HS_{VN}^c(t) = MeltMat^c(t) + HS_{VN}^c(t - 1). \quad (12)$$

Note that at the very end of the winter season the reference stations would eventually melt out, preventing any melting rates from being derived. In this case, the final melting rates before meltout have been used for the interpolation. In addition, negative values of  $HS_{VN}$  have been set to 0.

**3.2. Parameters of verification**

*HNW verification*

In order to validate the performance of  $HNW_{VN}$  at the control stations (in the following the index *c* is not included) by comparing to the point measurements  $HNW_{MEAS}$ , and to compare the results to the performance of other automatic methods, parameters of comparison were used (Egli and Jonas, 2009). The parameters are briefly summarized below.

1. Systematic bias  $\overline{\delta HNW}$ :

$$\overline{\delta HNW} = mean(HNW_{VN} - HNW_{MEAS}). \quad (13)$$

2. The absolute accuracy  $\sigma(\delta HNW)$ :

$$\sigma(\delta HNW) = standard\ deviation(HNW_{VN} - HNW_{MEAS}). \quad (14)$$

3.  $R_{log}^2$ : The coefficient of correlation ( $R_{log}^2$ ) between log-transformed  $HNW_{VN}$  and  $HNW_{MEAS}$ .
4. POD and FAR: Parameters adopted from severe weather forecast theory (Murphy and Winkler, 1987) have been used to detect certain classes of snowfall events, namely the probability of detection (POD) and the false alarm rate (FAR). To calculate POD and FAR, we used contingency tables (Table 2) for four classes of HNW intensity (Snow-NoSnow:  $HNW_{MEAS} \geq 0$  mm and  $< 1$  mm; Low:  $HNW_{MEAS} \geq 1$  mm and  $< 15$  mm; Medium:  $HNW_{MEAS} \geq 15$  mm and  $< 30$  mm; High:  $HNW_{MEAS} \geq 30$  mm).

The POD and FAR were calculated for every class using

$$POD = \frac{d}{b + d} \quad (15)$$

and

$$FAR = \frac{c}{c + d}, \quad (16)$$

where *b*, *c* and *d* were derived from the contingency table (Table 2).

5. Ranking points: A ranking point scale for the overall assessment relative to other HNW estimation methods was tested in Egli and others (2009). For each comparative measure as described above, the best performance was rated with 7 points and the lowest performance with 0 points. The different ranking points for each parameter and class were added.

*HS verification*

HS data from the VN ( $HS_{VN}$ ) were validated against  $HS_{MEAS}$  by applying the following parameters of comparison (Egli and Jonas, 2009), restricted to the control stations.

1. Systematic bias ( $\alpha$ ): The percent systematic bias  $\alpha$  was determined by a least-squares fit to

$$HS_{VN} = \alpha \times HS_{MEAS}, \quad (17)$$

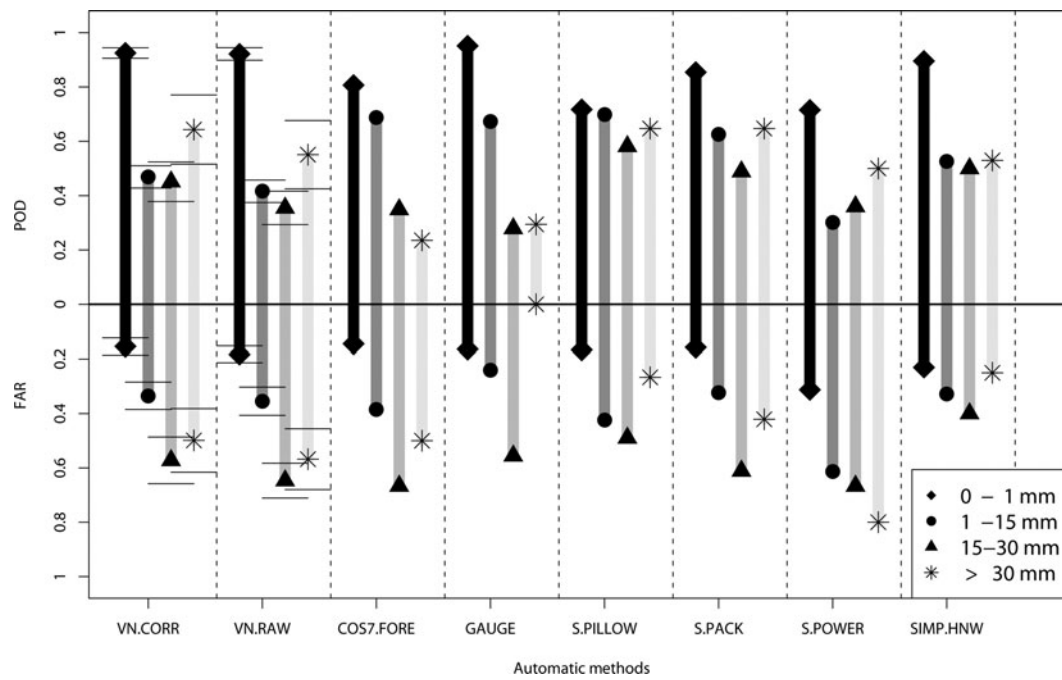


**Fig. 2.** POD and FAR values for the four different classes of HNW intensity (diamond, point, triangle, star). The values are listed either for single point measurements or the average of 106 control stations, where the error bars denote the deviation from the mean.

where the standard error of  $\alpha$  was also determined ( $error_{\alpha}$ ). Here,  $error_{\alpha}$  is a measure of the spread of the data around the fitting line.

2. Absolute error (RMSE): The averaged absolute difference between  $HS_{VN}$  and  $HS_{MEAS}$ , the root-mean-squared error (RMSE), was included in the comparison statistics:

$$RMSE = \sqrt{\frac{1}{N} \sum_{i=1}^N (HS_{VN}^i - HS_{MEAS}^i)^2}, \quad (18)$$

where  $i$  indexes one day of the analysed periods if either  $HS_{VN}^i > 0$  or  $HS_{MEAS}^i > 0$ . Since HS is investigated instead of SWE (Egli and others, 2009), a direct comparison of these studies by a ranking point score is not appropriate.

## 4. RESULTS AND DISCUSSION

### 4.1. HNW

Results of the validation of  $HNW_{VN}$  and  $HNW_{MEAS}$  are listed in Table 3 and presented in Figure 2. The parameters of comparison were calculated for both  $HNW_{VN.CORR}$  and  $HNW_{VN.RAW}$  compared to  $HNW_{MEAS}$ . For reference, they are listed together with corresponding results of other HNW estimation methods which were tested in Egli and others (2009). The parameters for VN.CORR and VN.RAW are averaged over all 106 control stations (Table 3:  $n_{stations}$ ), where the lines below and above the end of the vertical bars in Figure 2 (as well as the numbers in brackets in Table 3) represent  $\pm$ half of the standard deviation.

Table 3 summarizes the parameters for HNW comparison ( $\overline{\delta HNW}$ ,  $\sigma(\delta HNW)$  and  $R_{log}^2$ ) in order of the highest ranking points. While  $\overline{\delta HNW} < 0$  indicates a general underestimation of  $HNW_{VN}$  to  $HNW_{MEAS}$ ,  $\overline{\delta HNW} > 0$  denote a statistical overestimation. The results for VN.CORR and VN.RAW reveal a systematic bias close to 0. However, the considerably large deviation around the mean values of

**Table 3.** Comparative statistics to assess the performance of VN relative to competing methods tested in Egli and others (2009); notation of the systematic bias ( $\overline{\delta HNW}$ ), the absolute accuracy ( $\sigma(\delta HNW)$ ), the coefficient of correlation  $R_{log}^2$  and the ranking point system are described in section 3.2

Method	$n_{stations}$	$n_{days}$	$\overline{\delta HNW}$ mm	$\sigma(\delta HNW)$ mm	$R_{log}^2$	Ranking points
<b>VN.CORR</b>	<b>106</b>	<b>484</b>	<b>-0.03 (<math>\pm 0.35</math>)</b>	<b>4.01 (<math>\pm 0.62</math>)</b>	<b>0.78 (<math>\pm 0.037</math>)</b>	<b>51</b>
GAUGE	1	725	-1.15	4.12	0.89	50
SNOWPILLOW	1	719	0.6	4.41	0.79	49
SNOWPACK	1	726	0.6	5.07	0.82	48
SIMPLE-HNW	1	723	-0.68	5.04	0.8	45
<b>VN.RAW</b>	<b>106</b>	<b>484</b>	<b>0.22 (<math>\pm 0.47</math>)</b>	<b>4.89 (<math>\pm 0.65</math>)</b>	<b>0.72 (<math>\pm 0.035</math>)</b>	<b>30</b>
COSMO forecast	1	722	0.09	6.59	0.74	30
SNOWPOWER	1	348	2.59	15.37	0.41	5

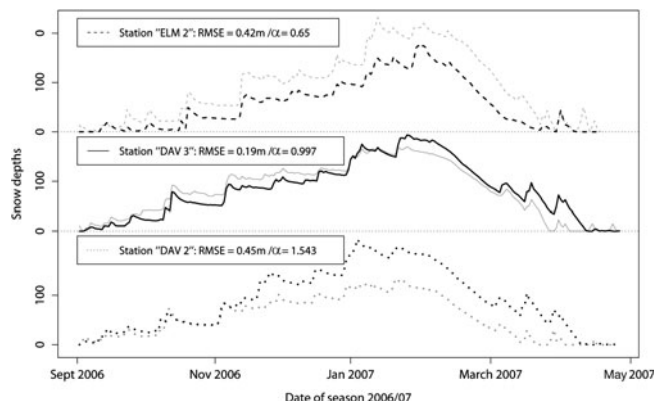


**Fig. 3.** The temporal development of snow depths derived by the virtual network (black curves) and the point measurements (grey curves) for three selected stations. The systematic bias ( $\alpha$ ) and the absolute error (RMSE) are indicated in the legend.

VN.CORR and VN.RAW indicates that some stations exhibit a large under-/overestimation of  $HNW_{VN}$ .

A more detailed analysis of the frequency distribution showed that the individual  $\delta HNW$ s at each control station are approximately equally distributed around the mean value of  $-0.03$  mm. This indicates an arbitrary character which stems from the comparison of the point measurements  $HNW_{MEAS}$  with data representing a much larger domain of estimation for  $HNW_{VN,CORR}$  or  $HNW_{VN,RAW}$ . This is supported by the fact that the stations are randomly distributed in a cuboid of  $7 \text{ km} \times 7 \text{ km}$  by  $500 \text{ m}$  (Schaub, 2007), which also explains why the deviations are generally similar for VN.CORR and VN.RAW.

For VN.CORR,  $\sigma(\delta HNW)$  demonstrates considerably small values for the mean ( $\sigma(\delta HNW) = 4.01 \text{ mm}$ ) with a deviation from the mean of about  $\pm 0.62$ . This low absolute error  $\sigma(\delta HNW)$  implies that, in principle,  $HNW_{VN,CORR}$  can also be calibrated for each single station of the measuring network. The systematic bias of each station can therefore be reduced, resulting in a lower deviation ( $\pm$ ) in  $\delta HNW$ . However, due to the comparison of a point measurement with a cuboid area, a calibration of  $HNW_{VN,CORR}$  is not meaningful. In fact, the values of  $HNW_{VN,CORR}$  may be considered as an average measurement of HNW over a large area, therefore representing a complementary network to the point measurements.

Taking the performance of SNOWPACK for  $\sigma(\delta HNW)$  as a benchmark, about 82% of the 106 control stations of the VN exhibit a  $\sigma(\delta HNW) < 5.07 \text{ mm}$ . The absolute accuracy between  $HNW_{MEAS}$  and  $HNW_{VN,CORR}$  is therefore comparable to the operational SNOWPACK-HNW estimations for manual reference measurements investigated at a single location. Note that SNOWPACK calculations are in operational use for Swiss avalanche warning (Rhyner and others, 2002) and provide different types of snowpack properties (Lehning and others, 2002). However, they are restricted to the locations of the IMIS network (Rhyner and others, 2002). In contrast, VN.CORR constitutes a complementary network over the entire Swiss Alps (although restricted solely to the HNW (and HS) estimation).

The POD/FAR statistics show that VN.CORR performs for all classes of intensities with better POD/FAR values than VN.RAW. Note that POD denotes the percentage of  $HNW_{MEAS}$ , also measured by  $HNW_{VN}$ , while FAR represents

the percentage of  $HNW_{VN}$  which are not observed by  $HNW_{MEAS}$ . VN.CORR has similar features to the POD/FAR statistics of SNOWPACK, in particular for the two highest classes of intensity (Medium and High) and for the Snow-NoSnow class, which are the most important for avalanche risk management decisions. The good performance of VN.CORR in POD/FAR statistics with respect to the Snow-NoSnow class also implies that COSMO-7 is capable of distinguishing between snow and rain. Note that results do not deteriorate if evaluated for the three elevation bands separately (data not shown).

Furthermore, the calibration routine to derive VN.CORR implies that at the reference station  $HNW_{VN,CORR} = HNW_{MEAS}$ , independent of the processes leading to  $HNW_{MEAS}$  such as combinations of solid, liquid precipitation and evaporation.

The low performance of VN.CORR in POD ( $\sim 0.45$ ) and FAR ( $\sim 0.35$ ) for the Low class diverges from the SNOWPACK results. In this class, VN.CORR is comparable to the performance of the SIMPLE-HNW method. This is unsurprising given that HNW are determined using SIMPLE-HNW at the control stations. This limits the potential of our approach to deal with situations in which the change in snow depth is strongly influenced by both snowfall and settling. While Equation (1) implicitly includes the effect of settling of new snow and the entire snow cover, it may become inaccurate after the first day of a multi-day snowfall event. In such situations VN.CORR therefore may not perform as well as a physical snowpack model. Note also that the difference in the time of measurements between the manual and automatic measurements (8 hours; see section 2) may lead to erroneous HNW estimates in a few cases (e.g. if a significant precipitation event occurs between 0000 and 0800 h). However, an HNW analysis of manual and automatic stations separately (data not shown) revealed very similar results with respect to POD/FAR statistics, which implies that this effect is minor.

Overall, VN.CORR demonstrates an advantage over VN.RAW. In particular, the calculation described by Equations (1–5) demonstrated the largest improvement. The method of removing the outliers has a minor impact on the results of VN.CORR. Moreover, in comparison to the other methods, VN.CORR yields the highest number of ranking points and therefore constitutes an adequate automatic estimation for HNW over the entire Swiss Alps.

#### 4.2. HS

Figure 3 shows the temporal development of the modelled HS ( $HS_{VN}$ , black curves) and the measured HS ( $HS_{MEAS}$ , grey curves) during winter 2006/07 for three exemplary locations of automatic measurement stations (ELM 2, DAV 2 and DAV 3). A temporal development of HS is first displayed where  $HS_{VN}$  describes a curve consistently below  $HS_{MEAS}$  (ELM 2), resulting in a systematic underestimation of  $\alpha = 0.65$  and a mean absolute error (RMSE) of  $0.42 \text{ m}$ . Secondly, a trajectory is shown (DAV 3) where the systematic bias ( $\alpha$ ) is close to 1 and  $RMSE = 0.19 \text{ m}$ , indicating a strong congruence between the curves. Finally, a station (DAV 2) is shown which describes a path constantly above  $HS_{MEAS}$ , resulting in  $\alpha = 1.54$  and  $RMSE = 0.45 \text{ m}$  (i.e. similar to that of ELM 2). Despite the fact that  $HS_{VN}$  shows considerable deviation from  $HS_{MEAS}$  for some stations, all stations generally reproduce the temporal progression qualitatively well. This is particularly true for the peaks

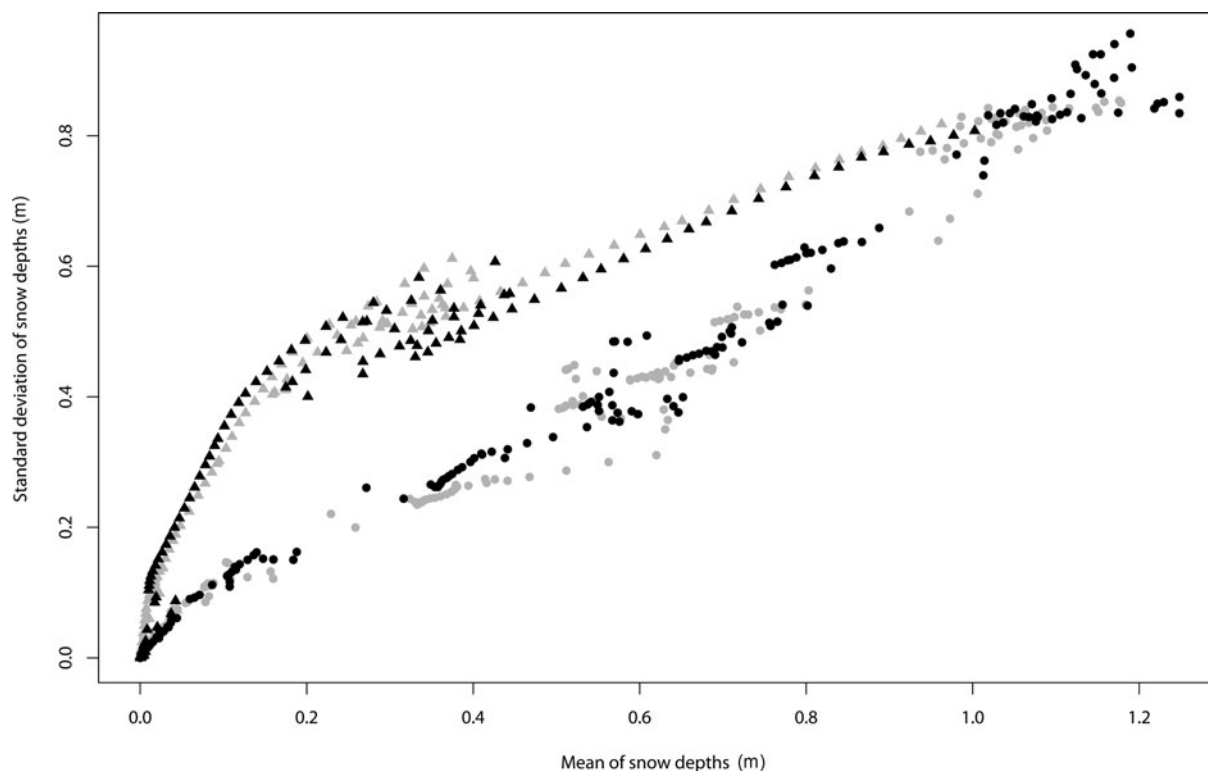


**Fig. 4.** The evolution of the mean snow depths ( $\overline{HS}$ ) and the standard deviation of snow depths ( $\sigma(HS)$ ) derived by the virtual network ( $HS_{VN}$ , black symbols) and the point measurements ( $HS_{MEAS}$ , grey symbols). The trajectory during the period of accumulation is indicated by points; the trajectory during ablation is indicated by triangles.

during accumulation and the following settling (produced by Equations (7) and (8)). The same result is obtained for the ablation derived by Equations (9–12).

Basically, the ablation period is generated by the VN only by means of differences of HS, where the melt rate matrix (Equation (8)) actually refers to a combination of some fresh snow accumulation, settling and melting. As the peaks are attributed to snow accumulation by daily new snowfall ( $HNW_{VN,CORR}$ ), the deviation from  $HS_{MEAS}$  stems from possible under-/overestimations of  $HNW_{VN,CORR}$ , as discussed in section 4.1. Analogous to the results and discussion of the systematic bias of  $HNW_{VN,CORR}$ , the specific values of  $\alpha$  for each station are approximately equally distributed around the mean value of  $\overline{\alpha} = 1.06 \pm 0.286$ . Accordingly, while  $\alpha$  is reasonably close to 1,  $\overline{error}_{\alpha} = 0.022 \pm 0.026$  and  $RMSE = 0.40 \pm 0.12$  m are very large (see Table 4).

### 4.3. Spatial analysis

Since the analysis of the single point measurements of  $HS_{VN}$  is limited due to its random nature, an investigation of  $HS_{VN}$  and  $HNW_{VN,CORR}$  regarding the Swiss Alps as an entire area

is also considered. First, the mean of all snow depths of point and VN estimations ( $\overline{HS_{MEAS}}$  and  $\overline{HS_{VN}}$ ) and their standard deviation ( $\sigma(HS_{MEAS})$  and  $\sigma(HS_{VN})$ ) are calculated. Figure 4 displays the evolution of  $\sigma(HS_{VN})$  with  $\overline{HS_{VN}}$  (black symbols) and  $\sigma(HS_{MEAS})$  with  $\overline{HS_{MEAS}}$  (grey symbols), where each point of the trajectory represents one day of the year 2006/07. The curves show a characteristic hysteretic dynamics as discussed in Egli and Jonas (2009). The trajectories of the period of accumulation (points) and ablation (triangles) are clearly separated. The quasi-linear increase of  $\sigma(HS_{VN})$  with increasing  $\overline{HS_{VN}}$  highlights that accumulation of snow leads to an increase in the differences between sites. The path during ablation, on the other hand, is mainly attributed to the spatial distribution of melting rates in the Alpine region.

It has been shown (Egli and Jonas, 2009) that the curves of the hysteretic dynamics are similar between years and therefore characterize the seasonal development of HS in the Swiss Alps. Figure 4 shows that both the periods of accumulation and ablation are well reproduced by  $HS_{VN}$  when compared to  $HS_{MEAS}$ . The seasonal characteristic of the HS development is therefore also displayed by the VN. We therefore speculate that  $HS_{VN}$  correctly reproduces the total

**Table 4.** The parameters of  $HS_{VN}$  evaluation statistics ( $\alpha$ ,  $error_{\alpha}$  and RMSE) as described in section 3.2 calculated either for the analysis per station averaged over 106 stations ( $HS_{VN}$  per station), or for the analysis of  $HS_{VN}$  averaged over all stations (average of  $HS_{VN}$ )

	$n_{stations}$	$n_{days}$	$\overline{\alpha}$	$\overline{error}_{\alpha}$	$\overline{RMSE}$
$HS_{VN}$ per station	106	782 ( $\pm 73$ )	1.06 ( $\pm 0.286$ )	0.022 ( $\pm 0.026$ )	0.40 ( $\pm 0.12$ )
Average of $HS_{VN}$	106	809	$\alpha$ of $\overline{HS}$ 0.96	$error_{\alpha}$ of $\overline{HS}$ 0.004	RMSE of $\overline{HS}$ 0.08

amount of snow depths during a season at Swiss Alpine scale. Moreover, when evaluating  $\alpha$ ,  $\text{error}_\alpha$  and RMSE for  $\overline{\text{HS}}_{\text{MEAS}}$  and  $\overline{\text{HS}}_{\text{VN}}$  (HS is averaged day by day over all stations), the percentage bias is as small as  $-4\%$  (Table 4).

Furthermore, the variogram analysis of HNW (Egli, 2008) showed that the statistical correlation length of HNW over the entire Swiss Alps is about 50–60 km. The same correlation length was found in Schaub (2007), analysing the raw HNW output of COSMO ( $\text{HNW}_{\text{VN.RAW}}$ ). This additionally supports the assumption that  $\text{HNW}_{\text{VN}}$  reproduces the regional precipitation patterns of the Swiss Alps appropriately and can be used as an input parameter for spatially distributed snow models.

Finally, the POD statistics of point HNW measurements as a function of the distance between two measuring sites (Egli, 2008) showed that, for the smallest scale (5–10 km), the POD is about 60% for HNW intensities more than 30 mm (High). The same value has been derived from a comparison of  $\text{HNW}_{\text{VN.CORR}}$  and  $\text{HNW}_{\text{MEAS}}$ . Again, a better performance of the VN HNW estimation in the POD statistics of two point measurement stations about 7 km distant would have been astonishing, since the large area of  $\text{HNW}_{\text{VN.CORR}}$  covers a gridcell of 7 km  $\times$  7 km. As the POD decreases rapidly with the distance from a point measurement station (Egli, 2008), the VN may also be applied for avalanche risk management warning for the locations between the point measurements where no HNW estimation is available.

## 5. CONCLUSION AND OUTLOOK

In this study, the HNW output of the numerical weather prediction model COSMO-7 was coupled with a simple snow accumulation/melting model in order to provide HNW/HS grids of 7 km resolution for the entire Swiss Alps. The results for the  $\text{HNW}_{\text{VN}}$  estimation showed that, on average, its performance is comparable to the performance of different automatic point measurements.  $\text{HNW}_{\text{VN}}$  therefore represents a complementary network for avalanche risk management applications and can also be used as input data for spatially distributed snow hydrological models where HNW is required.

This is also the case for the HS estimation by the VN, where the statistical dynamics of the mean of HS ( $\overline{\text{HS}}_{\text{VN}}$ ) and its standard deviation ( $\sigma(\text{HS}_{\text{VN}})$ ) are congruent to the measured dynamics. As a consequence, the estimations of HS by the VN over the entire Swiss Alps may be used to estimate the total amount of snow and snow water equivalent for larger catchments. At a local scale, however, a direct comparison of the point measurement to the corresponding gridcell of the VN may result in considerable deviation. This may stem from the fact that a measurement over a large area (7 km  $\times$  7 km for the VN) is compared to a single point measurement.

Future effort is necessary to investigate the spatial scales over which the VN is capable of providing a good performance for estimation of HNW/HS. For this purpose we will extend the application to COSMO-2, a new high-resolution version of COSMO available from February 2008 for a mesh size of 2.2 km. Additionally, the differences in the VN between the assimilation mode and the forecast mode of COSMO-2 will be investigated. Finally, the principle of the VN presented here can be applied to other regions which are less densely equipped with automatic or manual point measurement stations than the Swiss Alps. If point

measurement stations and a numerical weather prediction model are available, HNW and HS can be estimated with a refined accuracy for spatially larger extended regions for avalanche-risk and water-resources management.

## ACKNOWLEDGEMENTS

We thank D. Schaub and F. Schubiger for their support with the data acquisition and processing, and the external reviewer E. Brun for his constructive suggestions which helped to improve the manuscript.

## REFERENCES

- Anderton, S.P., S.M. White and B. Alvera. 2002. Micro-scale spatial variability and the timing of snow melt runoff in a high mountain catchment. *J. Hydrol.*, **268**(1–4), 158–176.
- Durand, Y., E. Brun, L. Mérindol, G. Guyomarc'h, B. Lesaffre and E. Martin. 1993. A meteorological estimation of relevant parameters for snow models. *Ann. Glaciol.*, **18**, 65–71.
- Egli, L. 2008. Spatial variability of new snow amounts derived from a dense network of Alpine automatic stations. *Ann. Glaciol.*, **49**, 51–55.
- Egli, L. and T. Jonas. 2009. Hysteretic dynamics of seasonal snow depth distribution in the Swiss Alps. *Geophys. Res. Lett.*, **36**(2), L02501. (10.1029/2008GL035545.)
- Egli, L., T. Jonas and R. Meister. 2009. Comparison of different automatic methods for estimating snow water equivalent. *Cold Reg. Sci. Technol.*, **57**(2–3), 107–115.
- Grayson, R. and G. Blöschl, eds. 2001. *Spatial patterns in catchment hydrology: observations and modelling*. Cambridge, etc., Cambridge University Press.
- Lehning, M., P. Bartelt, B. Brown, C. Fierz and P. Satyawali. 2002. A physical SNOWPACK model for the Swiss avalanche warning. Part II: snow microstructure. *Cold Reg. Sci. Technol.*, **35**(3), 147–167.
- Lehning, M., I. Völksch, D. Gustafsson, T.A. Nguyen, M. Stähli and M. Zappa. 2006. ALPINE3D: a detailed model of mountain surface processes and its application to snow hydrology. *Hydrol. Process.*, **20**(10), 2111–2128.
- Liston, G.E. and K. Elder. 2006. A distributed snow-evolution modeling system (SnowModel). *J. Hydromet.*, **7**(6), 1259–1276.
- Luce, C.H., D.G. Tarboton and K.R. Cooley. 1998. The influence of the spatial distribution of snow on basin-averaged snowmelt. *Hydrol. Process.*, **12**(10–11), 1671–1683.
- Marty, C. 2008. Regime shift of snow days in Switzerland. *Geophys. Res. Lett.*, **35**(12), 12501. (10.1029/2008GL033998.)
- McClung, D.M. and P.A. Schaerer. 1993. *The avalanche handbook*. Seattle, WA, The Mountaineers.
- Murphy, A.H. and R.L. Winkler. 1987. A general framework for forecast verification. *Mon. Weather Rev.*, **115**(7), 1330–1338.
- Rhyner, J. and 7 others. 2002. Avalanche warning Switzerland – consequences of the avalanche winter 1999. In Stevens, J.R., ed. *Proceedings of the International Snow Science Workshop 2002, 30 September–3 October 2002, Penticton, British Columbia*. Victoria, B.C., B.C. Ministry of Transportation. Snow Avalanche Programs.
- Schaeffli, B., B. Hingray and A. Musy. 2007. Climate change and hydropower production in the Swiss Alps: quantification of potential impacts and related modelling uncertainties. *Hydrol. Earth Syst. Sci.*, **11**(3), 1191–1205.
- Schaub, D. 2007. Vergleich realer IMIS Wetterdaten gegen COSMO-7 Modelldaten. (Diplomarbeit, Zürcher Hochschule für Angewandte Wissenschaften.)
- Skaugen, T. 2007. Modelling the spatial variability of snow water equivalent at the catchment scale. *Hydrol. Earth Syst. Sci.*, **11**(5), 1543–1550.